Inorg. Chem. **2009**, *48*, 1243−1249

Catalyst-Free Growth of Quasi-Aligned Nanorods of Single Crystal $Cu_3Mo_2O_9$ and Their Catalytic Properties

W. G. Chu,*,† H. F. Wang,*,† Y. J. Guo,† L. N. Zhang,‡,§ Z. H. Han,‡ Q. Q. Li,‡,§ and S. S. Fan‡,§

National Center for Nanoscience and Technology of China, Beijing 100085, P. R. China, Tsinghua-Foxconn Nanotechnology Research Center, Tsinghua University, Beijing 100085, P. R. China, and Department of Physics, Tsinghua University, Beijing 100085, P. R. China

Received October 3, 2008

We propose a simple and catalyst-free method to grow quasi-aligned single crystalline $Cu_3Mo_2O_9$ nanorods in terms of a mechanism differing from the conventional vapor−solid (VS) and vapor−liquid−solid (VLS) ones for chemical vapor deposition (CVD) methods by directly heating Cu foils in a mixed atmosphere of MoO_3 vapor and air. High quality $Cu_3Mo_2O_9$ nanorods can be simply grown in a temperature range from 450 to 550 °C whose diameter, length, and distribution density are dependent on both heating temperature and time. Interestingly, the growth rate at 550 °C drops significantly after 6 h. All nanorods grow along the [010] direction. On the basis of a proposed growth model, the nucleation of $Cu_3Mo_2O_9$ nanorods is believed to be governed by formation of initial polycrystalline Cu_xO protuberances with nanoscale diameters on Cu foils which may act as growth "templates". This novel method can be applied to grow other similar tertiary transition metal oxide nanostructures on substrates with large sizes. Most importantly, these $Cu_3Mo_2O_9$ nanorods decrease the ignition temperature of Printex U model soot from 600 to 438 °C, being in between 200 and 450 °C of the exhaust of diesel-powered combustion engines, which are therefore expected to be a potential efficient and environmentally friendly catalyst for diesel exhaust combustion.

Introduction

Numerous types of nanostructures can be grown in terms of the vapor−solid (VS) and vapor−liquid−solid (VLS) mechanisms for chemical vapor deposition (CVD) methods.[1−5] Growth and properties of one of the most important species, Mo-contained oxide nanostructures, especially binary ones, have been explored extensively due to their possible applications in catalysts, display devices, photochromisms, sensors, batteries, and smart windows.[6−11] A good case in point is molybdenum trioxide nanostructures, which can be used as catalysts, especially for deep oxidation of diesel exhaust soot.[12−14] However, few studies are reported on tertiary Mo-contained oxides so far.[15]

Tertiary copper molybdate $Cu_3Mo_2O_9$ is known to have an orthorhombic structure which can be described by the

* To whom correspondence should be addressed. E-mail: wgchu@nanoctr.cn (W.G.C.), hfwang@nanoctr.cn (H.F.W.).
† National Center for Nanoscience and Technology of China.
‡ Tsinghua-Foxconn Nanotechnology Research Center, Tsinghua University.
§ Department of Physics, Tsinghua University.

(1) Clark, T. E.; Nimmatoori, P.; Lew, K. K.; Pan, L.; Redwing, J. M.; Dickey, E. C. *Nano Lett.* **2008**, *8*, 1246–1252.
(2) Gundiah, G.; Deepak, F. L.; Govindaraj, A.; Rao, C. N. R. *Top. Catal.* **2003**, *24*, 137–146.
(3) Chu, W. G.; Zhang, L. N.; Wang, H. F.; Han, Z. H.; Han, D.; Li, Q. Q.; Fan, S. S. *J. Mater. Res.* **2007**, *22*, 1609–1617.
(4) Kodambaka, S.; Tersoff, J.; Reuter, M. C.; Ross, F. M. *Science* **2007**, *316*, 729–732.
(5) Wagner, R. S.; Ellis, W. C. *Appl. Phys. Lett.* **1964**, *4*, 89–90.
(6) Mestl, G. *Top. Catal.* **2006**, *38*, 69–82.
(7) Li, X. L.; Liu, J. F.; Li, Y. D. *Appl. Phys. Lett.* **2002**, *81*, 4832–4834.
(8) Ozin, G. A.; Özkar, S.; Prokopowicz, R. A. *Acc. Chem. Res.* **1992**, *25*, 553–560.
(9) Hamelmann, F.; Gesheva, K.; Ivanova, T.; Szekeres, A.; Abroshev, M.; Heinzmann, L. *J. Optoelectron. Adv. Mater.* **2005**, *7*, 393–399.
(10) Ajito, K.; Nagahara, L. A.; Tryk, D.; Hashimoto, A.; Fujishima, K. A. *J. Phys. Chem.* **1995**, *99*, 16383–16388.
(11) Wang, J. F.; Rose, K. C.; Lieber, C. M. *J. Phys. Chem. B* **1999**, *103*, 8405–8409.
(12) Braun, S.; Appel, L. G.; Schmal, M. *Catal. Commun.* **2005**, *6*, 7–12.
(13) Setten, B. A. A. L.; Spitters, C. G. M.; Bremmer, J.; Mulders, A. M. M.; Makkee, M.; Moulijin, J. A. *Appl. Catal., B* **2003**, *42*, 337–347.
(14) Leocadio, I. C. L.; Braun, S.; Schmal, M. *J. Catal.* **2004**, *223*, 114–121.
(15) Xu, J. S.; Xue, D. F. *J. Solid State Chem.* **2007**, *180*, 119–126.

10.1021/ic801885c CCC: $40.75
Published on Web 01/07/2009

space group *Pnma*.[16] Included in this unit cell are two types of almost regular Mo-4O tetrahedra, one type of compressed Cu-6O octahedral, and two types of Cu-5O polyhedra (see Supporting Information, Figure S1).[16] The Mo-4O tetrahedra with some bond lengths similar to those in MoO_3 make it possible for it to be a catalyst just like MoO_3, since catalytic properties of these metal oxides are closely related to metal−oxygen bonds. The complicated Cu−O polyhedra not only give rise to their complex magnetic transitions but may promote their performance as catalysts due to the incorporation of copper ions in the lattice.[17] In addition, the morphology and size of nanostructured catalysts usually have a significant influence on their catalyzing properties and efficiency. In this contribution, we propose a simple method to grow quasi-aligned arrays of tertiary single crystalline $Cu_3Mo_2O_9$ nanorods on Cu foils without catalysts involved which differs from the conventional VS and VLS methods. Influences of the reaction parameters on morphology and growth are explored in detail. Their good catalyzing properties as catalysts for soot combustion are tested, which renders nanostructured $Cu_3Mo_2O_9$ to be a potential efficient and environmentally friendly catalyst for diesel exhaust combustion.

Results and Discussion

Morphology and Structure of $Cu_3Mo_2O_9$ Nanorods. Growth experiments were carried out at 400, 450, 500, 550, 600, 650, and 700 °C for various times, respectively. Rod-like products were successfully grown at all temperatures except at 400 and 700 °C, and some of their scanning electron microscopy (SEM) and energy dispersive X-ray spectroscopy (EDS) images are shown in Figure 1. Quantitative analysis of EDS shown in Figure 1i gives a chemical stoichiometry of $Cu_3Mo_{2.11}O_{8.52}$. To determine the crystal structure of the nanorods, X-ray diffraction (XRD) experiments on the typical sample grown at 550 °C for 24 h (Figure 1i) were carried out. However, we failed to identify its crystal structure due to the absence of many reflections arising from the quasi-alignment of nanorods at the surface of copper foils. Then, we collected these nanorods by slightly ultrasonicating these copper foils for the phase identification. The typical powder XRD pattern is shown in Figure 2. The structure is unambiguously identified as orthorhombic $Cu_3Mo_2O_9$ (JCPDS: 87-0455),[16] being consistent with the chemical analysis of EDS. From the XRD pattern the powder is found to be mostly comprised of crystalline $Cu_3Mo_2O_9$. Structures of the samples grown under other conditions were also identified as orthorhombic $Cu_3Mo_2O_9$ by careful transmission electron microscopy (TEM) observations and electron diffraction (ED) analysis.

It can be seen from Figure 1 that the distribution density and diameter of as-grown rods tend to increase with increased times at both 450 and 550 °C. The rod-like products grown at 600 °C for 24 h were significantly coalesced, and thus the distribution density reduced. Careful inspection revealed some traces of "remelting" of products which resulted in smooth surfaces. By further increasing the growth temperature up to 650 °C, both the density and the diameter of products decrease greatly, and traces of the "remelting" seem more obvious for the 24 h growth. However, at 700 °C for 24 h, no rod-like products are visible.

By comparing the morphology and size of products grown at the temperatures studied, 550 °C is found to be the optimum growth temperature. The insets in Figure 1 clearly show a fairly uniform distribution of rod lengths at 550 °C, and the average length tends to increase with increased growth times ranging from about 8.0 μm for 2 h to 20.5 μm for 24 h. To get further information on the growth kinetics at 550 °C, we derived the distribution of diameters of rods for various growth times as well, which is shown in Figure 3.

The diameters of rods are found to have a broad and asymmetrical distribution ranging from a few tens of nanometers to 2 μm with a relatively long tail on the side of larger diameters, though these are very small in percentage, especially for longer growth times. However, most of the rods are still of nanometer size, even for long time growth. Also, the distribution of diameters tends to get broader with increased growth times. The diameter distributions allow us to obtain the average diameters from which the average volumes are derived combined with the average lengths. The average diameters and volumes are plotted against growth times in Figure 3g. Interestingly, time dependencies of the average diameters and volumes of rods for the durations studied show two distinct linear regions, which are crossed at about 6 h. For less than 6 h, the increase rates in diameter and volume are 53.0 nm/h and 0.7 μm^3/h, respectively, whereas they are 6.0 nm/h and 0.2 μm^3/h, respectively, for more than 6 h. This clearly reveals that the growth slows down after 6 h.

Here, TEM, high resolution TEM (HRTEM), and ED are combined to characterize the growth behavior and detailed structure of nanorods grown under different conditions. Likewise, the sample grown at 550 °C for 24 h is taken as an example and is shown in Figure 4. ED shows that all of these nanorods are of single crystal. The combination of TEM and ED allows us to conclude that nanorods grow along [010]. From the experimental HRTEM image, no considerable defects are visible, suggesting good crystallinity. HRTEM image simulation along the $[\bar{3}01]$ crystal axis of the $Cu_3Mo_2O_9$ structure was made using dynamic electron diffraction theory,[18] in good agreement with experiment, as shown by the inset in Figure 4b.

Growth of Single Crystal $Cu_3Mo_2O_9$ Nanorods. To explore the growth of $Cu_3Mo_2O_9$ nanorods, the EDS line was scanned along numerous individual $Cu_3Mo_2O_9$ nanorods, and the spotted EDS spectra of rod-free zones around them were acquired, one of which is shown in Figure 5 for the sample grown at 550 °C for 24 h. Examination of the EDS output shows that almost no traces of Mo are detectable in the rod-

(16) Steiner, U.; Werner, R. *Acta Crystallogr., Sect. C* **1997**, *53*, 1371–1373.
(17) Hamasaki, T.; Tomoyuki, I.; Haruhiko, K.; Tomoyuki, S. *Phys. Rev. B* **2008**, *77*, 134419–134425.
(18) Cowley, J. M.; Moodie, A. *Acta Crystallogr.* **1957**, *10*, 609–619.

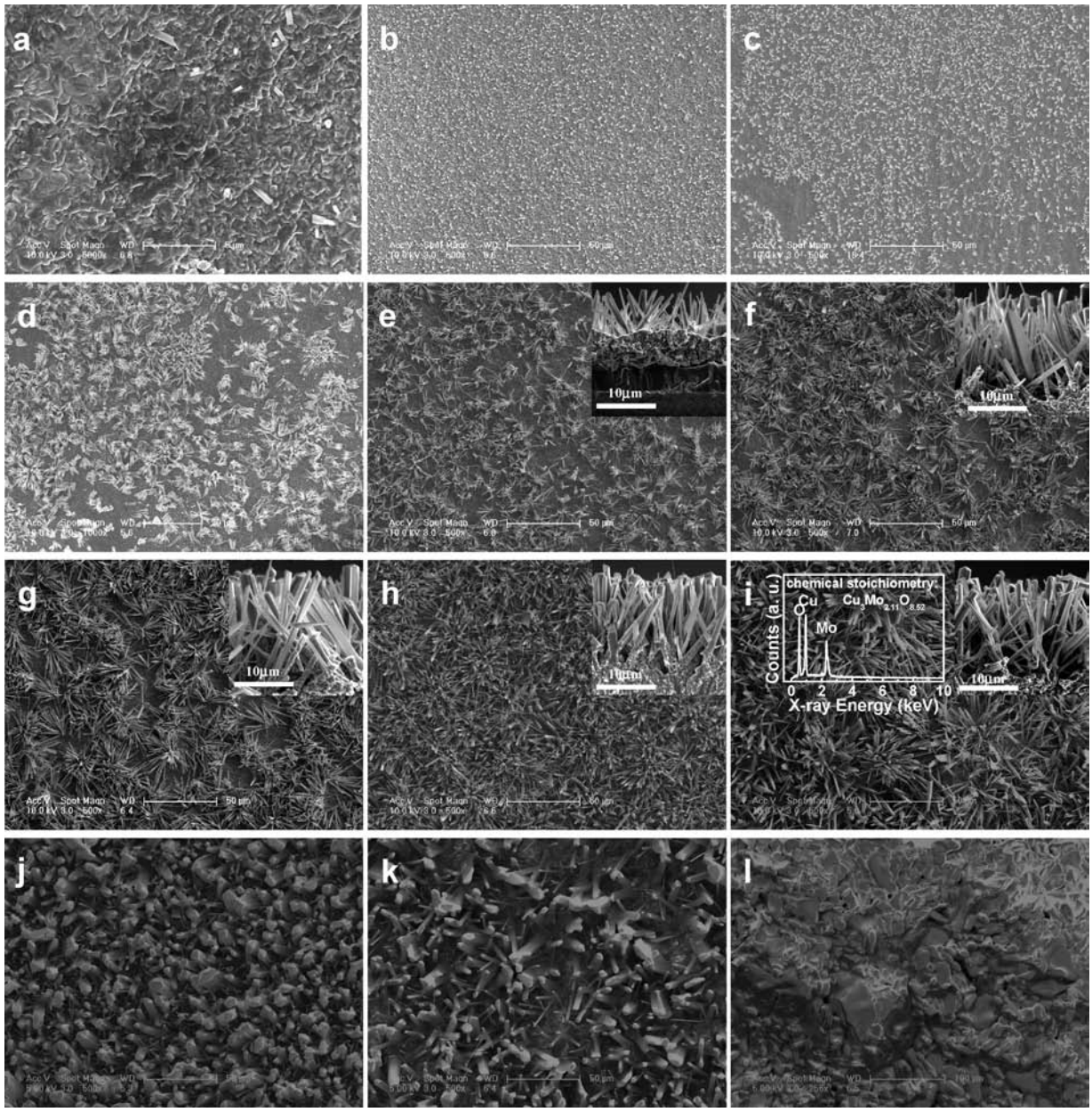

Figure 1. SEM images of nanorods grown at different temperatures for various times: (a−d) at 450 °C for 2, 4, 10, and 24 h, respectively; (e−i) at 550 °C for 2, 4, 6, 10, and 24 h, respectively; and (j−l) for 24 h at 600, 650, and 700 °C, respectively.

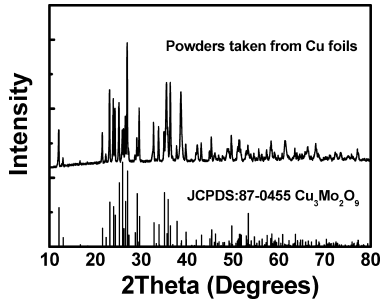

Figure 2. XRD patterns for $Cu_3Mo_2O_9$.

free zones. One nanorod is found to have two distinct parts, very rough surfaces and smooth surfaces, as indicated by Figure 5. Variations of Cu Lα, O Kα, and Mo Lα intensities along the nanorod also imply that two remarkably different regions with different chemical constituents correspond well to the above two parts with different morphologies, as observed by SEM. Changes of Mo Lα and O Kα intensities along a nanorod clearly show two platforms in which almost no Mo signals are seen across its root region, whereas the Cu Lα intensity across the root region is higher. The Mo-contained region has already been identified as single crystal $Cu_3Mo_2O_9$ in the above text. Also, the ratio of Cu Lα to O Kα intensities in the Mo-free root region is much higher than that in the single crystal $Cu_3Mo_2O_9$ nanorod region, as shown by Figure 5b. If the average ratio of Cu Lα to O Kα intensities, about 1.3, in the $Cu_3Mo_2O_9$ nanorod is reasonably assumed to correspond to an atomic ratio of Cu:O = 1:3 for $Cu_3Mo_2O_9$, the one, about 3.0, in the root region will give an estimate of a chemical stoichiometry of Cu:O = 0.77:1, close to CuO. As far as the rough morphology of the root region is concerned, it is probably composed of polycrys-

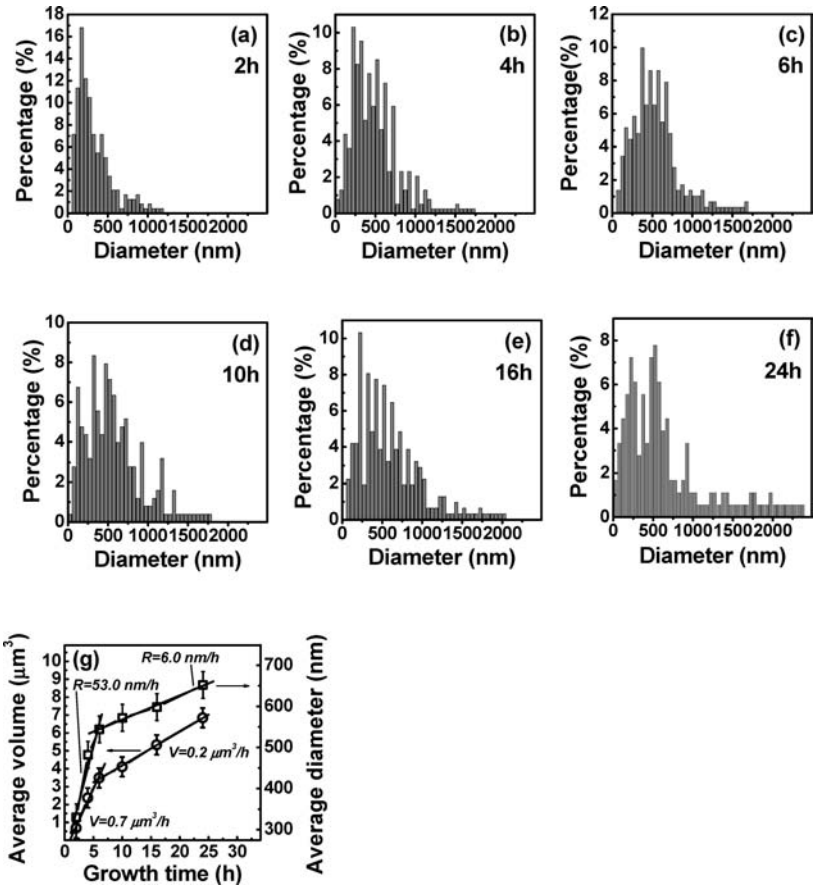

Figure 3. Distributions of diameters with various growth times at 550 °C (a−f) and growth time dependence of average diameter and volume (g), noting the two remarkably different rates of increase in both diameter and volume during the growth durations studied.

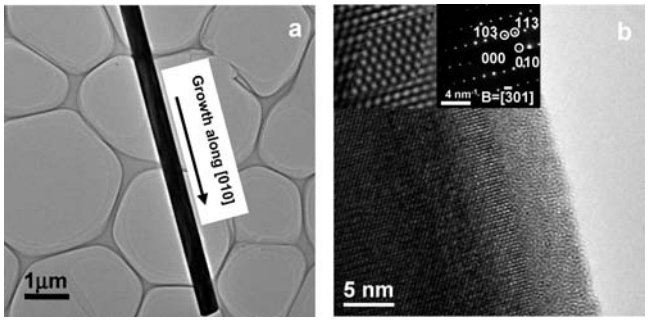

Figure 4. TEM, ED, and experimental and simulated HRTEM images of a nanorod grown at 550 °C for 24 h. A combination of ED and TEM reveals that nanorods grow along [010]. HRTEM experiment and simulation made with a thickness of 21.8 nm and a defocus of −170 nm agree very well.

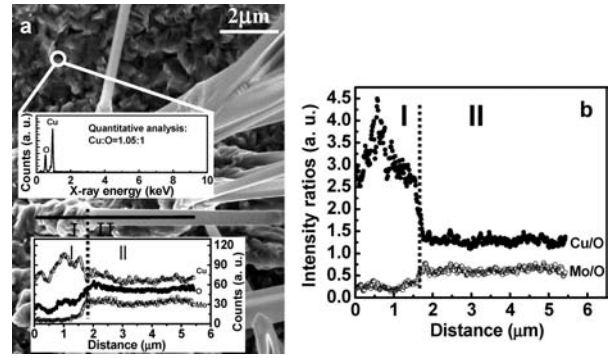

Figure 5. Variations of integrated intensities of Cu Lα, O Kα, and Mo Lα peaks derived from the EDS line scanned along one single $Cu_3Mo_2O_9$ nanorod from the sample grown grown at 550 °C for 24 h and the EDS of a nanorod-free zone. Note that there are almost no Mo traces detectable in the nanorod-free zone, and the intensity ratio of Cu to O in zone I is much higher than that in zone II.

talline Cu_xO crystallites. One-dimensional nanostructures are usually considered to grow in terms of the VLS and VS mechanisms.[19,20] The VLS mechanism is usually characterized by the presence of a catalyst (metal droplet) at the tip of one single nanowire or nanorod and the VS mechanism by evaporating materials in the higher temperature region followed by the growth of nanostructures in the lower temperature region. In this study, no catalyst-like particles were observed at the tip of single crystal $Cu_3Mo_2O_9$ nanorods. Also, the separations between the Cu foils and the MoO_3 sources during growth are very small, not more than 1.0 cm, and just the depth of one alumina boat (see Figure 8), implying no noticeable temperature difference between them. Therefore, the above two mechanisms are not responsible for the growth of single crystal $Cu_3Mo_2O_9$ nanorods.

It has been reported that CuO nanowires or -rods could be grown on Cu foils or other thin Cu substrates by annealing in an oxygen or air atmosphere.[21−24] However, the definite growth mechanisms are not clear yet. In the current study,

(19) Geng, C.; Jiang, Y.; Yao, Y.; Meng, X.; Zapien, J. A.; Lee, C. S.; Lifshitz, Y.; Lee, S. T. *Adv. Funct. Mater.* **2004**, *14*, 589–594.

(20) Wang, Z.; Zhao, Q.; Zhang, Y.; Xiang, B.; Yu, D. P. *Eur. Phys. J. D* **2005**, *34*, 303–305.

(21) Xu, C. H.; Woo, C. H.; Shi, S. Q. *Chem. Phys. Lett.* **2004**, *399*, 62–66.

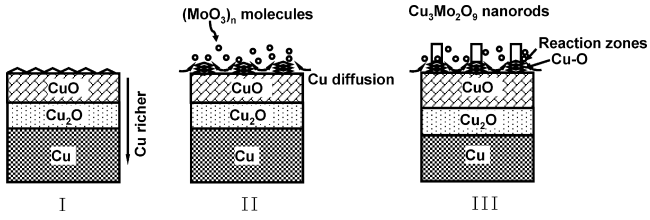

Figure 6. Growth model of single crystal $Cu_3Mo_2O_9$ nanorods. Phase I is the oxidation of surface of Cu foils; phase II is the formation of polycrystalline Cu_xO protuberances with nanoscale diameters; and phase III is the nucleation and growth of $Cu_3Mo_2O_9$.

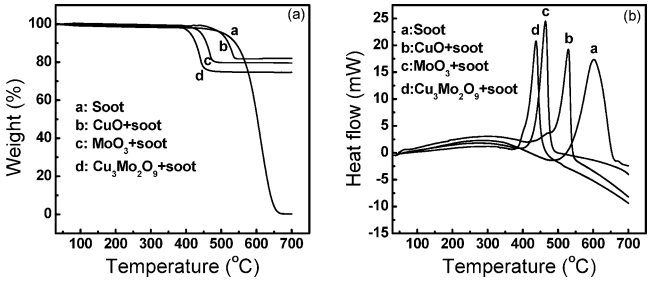

Figure 7. TG (a) and DTA (b) curves of soot, CuO + soot, MoO_3 + soot, and $Cu_3Mo_2O_9$ + soot.

the Cu foils were actually placed in a mixed atmosphere composed of vapor of MoO_3, due to its sublimation, and air. The experiments with Cu foils only in air for the same temperatures were also carried out, and CuO nanowires or -rods were successfully grown at 450, 500, 550, 600, and 650 °C as well. The temperature range in which $Cu_3Mo_2O_9$ nanorods can be grown coincides with that of CuO nanowires or -rods. This, together with the absence of Mo in both the nanorod-free zones and the root regions of nanorods, may give us a hint that the presence of vapor of MoO_3 alone does not greatly influence the nucleation of $Cu_3Mo_2O_9$ nanorods. It may be be governed by the same factors that determine the nucleation of the polycrystalline Cu_xO root regions with nanoscale diameters. These root regions may be taken as "templates" for the following nucleation and growth of single crystal $Cu_3Mo_2O_9$ nanorods. In our case, the similar root regions were also observed in the growth of CuO nanowires or -rods with Cu foils in air.

On the basis of the above experimental observations, a growth model is proposed and schematically illustrated in Figure 6. The growth of $Cu_3Mo_2O_9$ nanorods could be described as three phases: Phase I is the oxidation of surfaces of clean Cu foils forming layers of polycrystalline copper oxides such as CuO, usually with Cu_2O underneath. Surfaces may be characterized by many protuberances resulting from copper oxide crystallites. Phase II is the formation of the polycrystalline Cu_xO root regions with very rough surfaces driven by stresses introduced by the volume expansion due to formation of copper oxides and by built-in stresses in the copper foils. Phase III is the nucleation and growth of single crystal $Cu_3Mo_2O_9$ nanorods at the tips of rough Cu_xO root regions through the reaction between solid Cu_xO and MoO_3 vapor, accompanied by Cu diffusion.

According to the above model, the growth kinetics of $Cu_3Mo_2O_9$ nanorods is dictated by availability of Cu_xO and MoO_3 molecules. Actually, MoO_3 vapor exists in the form of $(MoO_3)_n$ (usually $n = 3-5$) molecules.[25] In this study, the growth temperatures are not so sufficiently high that Cu would reach reaction fronts via diffusions along surface, subgrain boundaries and dislocations instead of volume diffusion.[26] The directional diffusion is considered to be driven by the stresses yielded by volume expansion due to the formation of copper oxides ($V_{CuO}:V_{Cu_2O}:V_{Cu} = 1.73:1.64:1$) and by the built-in stresses in the copper foils during their processing. MoO_3 molecules which reach the surface of Cu foils may take part in the reaction mainly via surface diffusion as well. Interfaces between root regions and $Cu_3Mo_2O_9$ nanorods would be the dominant reaction sites for Cu_xO and $(MoO_3)_n$ molecules.

The pressure of MoO_3 vapor is strongly dependent on temperature and is 5.0×10^{-8}, 1.0×10^{-6}, 5.0×10^{-5}, 8.0×10^{-4}, 1.0×10^{-2}, and 1.1×10^{-1} Torr at 450, 500, 550, 600, 650, and 700 °C, respectively.[27] Cu diffusion is also enhanced as the growth temperature increases. It is reasonable that the growth rate is greater at higher temperatures. However, for too high temperatures, say 700 °C, the vapor pressure of MoO_3 increases almost exponentially so that too many MoO_3 molecules per unit time are provided, whereas no sufficient Cu is available. As a result, MoO_3 molecules would rapidly react with copper oxides at the whole surfaces of Cu foils to result in disappearance of nanorods with formation of uniform layers of Mo−Cu−O compounds, as Figure 1i shows. The abrupt decrease of the growth rate after 6 h could be ascribed to two factors: the increase in density of $Cu_3Mo_2O_9$ nanorods and the "passivation" of MoO_3 sublimation with time. A critical density may be reached after the growth for 6 h over which the effective number of $(MoO_3)_n$ molecules participating in reactions decreases significantly as a result of the shielding effect of nanorods caused by collisions and so forth. Meanwhile, the increase in density would also lead to the decrease of the number of $(MoO_3)_n$ molecules available for each nanorod, resulting in the slower growth rate. On the other hand, heating for 6 h at 550 °C may also cause the abrupt and rapid passivation of MoO_3 sublimation, somewhat suddenly slowing down the growth of $Cu_3Mo_2O_9$ nanorods.

Single crystal $Cu_3Mo_2O_9$ nanorods are unambiguously determined to grow along the [010] direction, which is closely related to its crystallography. The total amounts of Cu−O and Mo−O bonds along the [010] and [100] directions are 13 (nine Cu−O and four Mo−O bonds) and 11 (nine Cu−O and two Mo−O bonds), respectively, whereas

(22) Kaura, M.; Muthea, K. P.; Despandeb, S. K.; Choudhuryc, S.; Singhd, J. B.; Vermae, N.; Guptaa, S. K.; Yakhmi, J. V. *J. Cryst. Growth* **2006**, *289*, 670–675.
(23) Jiang, X. C.; Herricks, T.; Xia, Y. N. *Nano Lett.* **2002**, *2*, 1333–1338.
(24) Xu, C. H.; Woo, C. H.; Shi, S. Q. *Superlattices Microstruct.* **2004**, *36*, 31–38.
(25) Zang, A. *Physics at Surfaces*; Cambridge University Press: Cambridge, 1990; Chapter 15, p 400.
(26) Chen, J. T.; Zhang, F.; Wang, J.; Zhang, G. A.; Miao, B. B.; Fan, X. Y.; Yan, D.; Yan, P. X. *J. Alloys Compd.* **2008**, *454*, 268–273.
(27) Smolik, G. R.; Petti, D. A.; Schuetz, S. T. *Oxidation, Volatilization, and Redistribution of Molybdenum from TZM Alloy in Air*; Technical Publication for U. S. Department of Energy, Office of Energy Research: Idaho Falls, ID, January 2000; p 17.

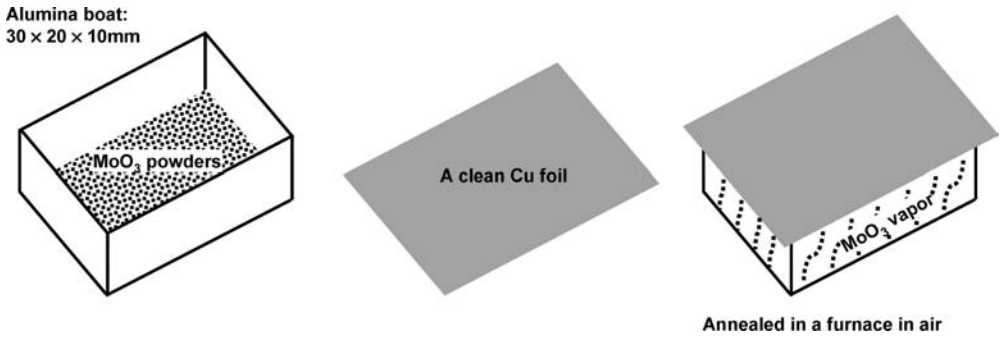

Figure 8. Schematic illustration for experimental assembly.

there are only eight Cu−O bonds with the average length of 2.244 Å along [001]. The average bond lengths for the Cu−O bonds along [010] and [100] are 1.918 and 2.105 Å, respectively. In contrast, the average length for the Mo−O bonds of the former (1.789 Å) is about 0.048 Å, a bit greater than that of the latter (1.741 Å). Therefore, the Cu−O bonds which account for the majority of bonds along [010] are by far shortest and greatest in number, as opposed to those along [100] and [001]. On the other hand, Cu−O octahedra form the stable and rigid network structure by sharing their corners along [010] and edges of neighboring Cu−O polyhedra. Therefore, more energy would be needed to break the bonds along [010]. On the contrary, the growth along this direction would release more energy so that the system is more stable. Consequently, $Cu_3Mo_2O_9$ nanorods would preferentially grow in the [010] direction from the perspective of energetics.

Catalytic Properties of $Cu_3Mo_2O_9$ Nanorods. We also attempted to test the catalyzing performance of $Cu_3Mo_2O_9$ nanorods. The thermogravimetry (TG) and differential thermal analysis (DTA) curves of $Cu_3Mo_2O_9$ + Printex U, Printex U, CuO + Printex U, and MoO_3 + Printex U are shown for comparison in Figure 7. It is seen that they are capable of lowering the combustion temperature of Printex U from 600 to 532 °C (CuO) and 466 °C (MoO_3) and further to 438 °C ($Cu_3Mo_2O_9$), respectively, in between 200 and 450 °C of the temperature range of the exhaust of diesel-powered combustion engines.[28] The higher activity of $Cu_3Mo_2O_9$ makes $Cu_3Mo_2O_9$ and MoO_3 competent catalysts for soot oxidation, which can be ascribed to the easier charge transfer among Cu, O, and Mo ions due to the introduction of Cu in the lattice compared to MoO_3. The likely process of charge transfer may be described as follows: First, soot reduces Cu^{2+} to Cu^{+} accompanied by formation of CO_2. Then, an electron is transferred from Cu^{+} to Mo^{6+} with the restoration of Cu^{2+}. Finally, Mo^{5+} is oxidized to Mo^{6+} again by oxygen. This kind of high activity of $Cu_3Mo_2O_9$ catalysts without chloride additives will be environmentally friendly as opposed to other catalysts promoted with chloride additives.[28] It is also noted that CeO_2 can be used as a catalyst for soot oxidation.[29] For the identical kind of soot, CeO_2 use decreases its oxidation temperature to about 500 °C, which is higher than 438 °C in the case of $Cu_3Mo_2O_9$.[29] Moreover, by further tailoring the morphology, size, and structure, $Cu_3Mo_2O_9$ is expected to be a potential efficient and, more importantly, environmentally friendly catalyst for diesel exhaust combustion. Further work is under way.

(28) Mul, G.; Neeft, J. P. A.; Kapteijin, F.; Makkee, M.; Moulijin, J. A. *Appl. Catal., B* **1995**, *6*, 339–352.
(29) Atribak, I.; Bueno-López, A.; García-García, A. *J. Catal.* **2008**, *259*, 123–132.

Conclusions

A simple, catalyst-free method was developed to successfully grow quasi-aligned nanorods on Cu foils by heating them in a mixed atmosphere of MoO_3 vapor and air in the temperature range from 450 to 650 °C. As-grown nanorods were identified to be single crystal $Cu_3Mo_2O_9$, and their growth direction was determined to be along the [010] direction. The diameter, length, and distribution density tend to increase as growth time and temperature increase. At 550 °C, the growth rate exhibits a turning point at about 6 h after which the increase rate of average volume decreases by a factor of about 3. The growth of $Cu_3Mo_2O_9$ nanorods was governed by formation of polycrystalline Cu_xO protuberances with nanoscale diameters on Cu foils which act as their "templates". This method could be used to grow aligned nanorods of other similar tertiary transition metal oxides on a large area of substrates. At present, we have successfully grown $Cu_3Mo_2O_9$ on copper substrates with a diameter of more than 10 cm. Most interestingly, $Cu_3Mo_2O_9$ is found to have high catalyzing activity for soot oxidation, which reduces the oxidization temperature of soot from 600 to 438 °C, and therefore expected to be a potential efficient and environmentally friendly catalyst for diesel exhaust combustion.

Experimental Section

MoO_3 powders with 99.99% purity (Beijing Chemical Reagents Company) were used as one of the ingredients to synthesize nanorods of $Cu_3Mo_2O_9$. Copper foils with 99.9% purity and a thickness of about 100 μm (Sinopharm Chemical Reagents Co. Ltd.) served as the other reaction ingredient and the substrate for supporting the resulted products. All copper foils were rinsed in a solution of 1 mol of nitridic acid for 5 min to remove the oxides at the surface, then supersonicated for 10 min in deionized water immediately, and finally dried in the flow of air. A rectangular alumina boat was used as a container in which a certain amount of MoO_3 powders was scattered on its inner bottom uniformly. Then a piece of copper foil with a larger size than the opening boat was covered on top of the boat, as illustrated in Figure 8. Finally, this assembly was placed into a furnace for heating for different times at various temperatures in air. After being heated and cooled down

to room temperature (RT), the original copper foils may look green-yellowish if $Cu_3Mo_2O_9$ nanorods were successfully grown. After each experiment, the remnants of MoO_3 powders were still visible in the alumina boat.

The morphology and structure of as-grown products were examined with field emission scanning electron microscopy (FES-EM, Sirion 200, FEI, U.S.A.) and HRTEM (Tecnai F20 G^2, S-twin, FEI, U.S.A.). TEM and HRTEM observations were made at an operation voltage of 200 kV. EDS was used to probe the chemical constituents of products.

Powder samples were collected by slightly ultrasonicating copper foils for XRD experiments on a diffractometer (Rigaku D/max 2500, Japan) with 40 kV and 200 mA (Cu radiation) and for test of catalyzing performance using TG and DTA (Diamond TG-DTA, Perkin-Elmer, U.S.A.). Printex U (Degussa, Germany) carbon black is taken as model soot for catalytic experiments. The sample weight used for TG and DTA experiments is about 5 mg $\pm$ 0.1 mg. The weight ratio between $Cu_3Mo_2O_9$ and Printex U in the mixtures is 3:1, and the others are about 4:1. Both TG and DTA experiments were carried out in air with a scan rate of 5 °C/min.

Acknowledgment. This work was funded by the Ministry of Science and Technology of China, Project 973 under Grant 2006CB932602.

Supporting Information Available: Details about the crystal structure of $Cu_3Mo_2O_9$ and schematic illustration. This material is available free of charge via the Internet at http://pubs.acs.org.

IC801885C